We are IntechOpen, the world's leading publisher of Open Access books Built by scientists, for scientists

6,900
Open access books available

186,000
International authors and editors

200M
Downloads

Our authors are among the

154
Countries delivered to

TOP 1%
most cited scientists

12.2%
Contributors from top 500 universities

CLARIVATE ANALYTICS
BOOK CITATION INDEX
INDEXED

WEB OF SCIENCE™

Selection of our books indexed in the Book Citation Index
in Web of Science™ Core Collection (BKCI)

Interested in publishing with us?
Contact book.department@intechopen.com

Electrochemical Formation of Silver Nanoparticles and Nanoclusters on Multiwall Carbon Nanotube Electrode Films

Andrés Alberto Arrocha Arcos and
Margarita Miranda-Hernández

Additional information is available at the end of the chapter

Abstract

The Ag nanoparticles and nanoclusters (AgNP, AgNC) have been widely used due to their multiple applications, for example, in catalysts for CO_2 to CO electrochemical reduction, O_2 reduction in fuel cells, interface design for plasmonic resonance experiments and H_2O_2 or glucose sensors. The chemical methods most used to obtain AgNP, reported in the literature are: borohydride reduction, the Tollens method or the sonication at high concentrations of $AgNO_3$. One important disadvantage of these methods is the multiple steps required for electrode design, especially in carbon materials, and one of them is MWCNTs, used in some applications mentioned above. Electrodeposition has been reported in the preparation of metallic particles. In this chapter, we described the electropolishing method in the preparation of AgNP and AgNC supported on MWCNT film. An advantage of this proposed method is that it allows obtaining AgNP and AgNC in situ, supported on carbon matrices, ready to use as electrodes in different applications.

Keywords: silver nanoparticles, silver nanoclusters, electropolishing method, multiwall carbon nanotubes, carbon film electrode

1. Introduction

Ag nanoparticles (AgNP) have been widely used in multiple applications related to energy and storage, in the electrocatalytic conversion of CO_2 to CO [1]; in the spectroscopic analysis by enhancing the plasmonic resonance effect [2]; in the environmental remediation by

degrading highly toxic compounds [3]; for biosensor design with H_2O_2 detection systems [4], and in many molecular interaction technologies with DNA, RNA and proteins [5].

Different methods for the synthesis and preparation AgNP have been reported; one of the most implemented technologies is the physical methods based on evaporation-condensation and laser ablation; these methods offer high reproducibility and no chemical contamination. The AgNP size achieved by the physical methods is around 10–100 nm layers [6, 7].

The chemical methods normally used convey a reduction step; one of the most widely used is the borohydride reduction in which the injection method is preferred to provide AgNP of 17 ± 2 nm by using a polymeric template [8, 9]. In the borohydride method, the silver cation is reduced by the free electron pairs on borohydride molecule [10, 11]. In the same way, the Tollens reagent for $[Ag(NH_3)_2]^+$ reduction with saccharides is a chemical reduction method; this method allows 50 nm as the smallest size by controlling the ammonia and saccharide concentration [12–14].

Other methods, as the assisted methods, implement techniques of radiation like the photoinduced method in which AgNP are synthesized with Ag^+ by exposure to UV light and nucleate around a polymer matrix as polyvinyl alcohol. Other polymers as carboxymethylated chitosan or Triton molecules allows AgNP synthesis by changing the light intensity [15]. Similar to this UV light, the microwave-assisted synthesis is possible using the same reducing agents and the same silver ion source [16]. Finally, the greener methods are based on the reduction principle by the implementation of polymers and polysaccharides. These methods are similar to the chemical reduction technologies; nevertheless, the reduction is performed in a biodegradable polymer source like starch and the reaction is performed in mild conditions [17, 18].

The biological organism like bacteria, fungi, algae and plants allows the synthesis of silver nanoparticles in mild conditions. Nevertheless, these organisms need to be tolerant to the presence of silver on water. Moreover, these syntheses are in the real sense working as the previously discussed chemical and polymer-assisted methods. Biological-assisted synthesis is complex but in general terms the living organism provides several reducing agents or templates for silver cations as example proteins and peptides provide several amino acids with free electron pairs as Tyr residues and carboxyl groups in Asp/Glu residues [19], enzymes like Cyt C, NADH-dependent reductase, nitroreductase are able to transfer electrons and reduce free silver cations [20–22]. Different cells which produce polysaccharides in the cell's wall are perfect nucleation sites for silver proliferation. Also, chitosan and other biopolymers are suitable as templates for particle arrangement. In the case of plants and algae, the plethora of organic xenobiotics is cumbersome, and many molecules as flavonoids, catechols and polyphenols are able to reduce silver [23, 24].

In the previous paragraphs, different methods have been described for the synthesis of AgNPs. However, in the practical use of nanomaterials, some difficulties must be overcome; one of them is to avoid the formation of aggregates when they are handled directly. The presence of aggregates often overrides their unique functionalities. Therefore, it is very important to implement immobilization techniques for metallic NPs on easily handled supports.

The immobilization of AgNP into several matrices of synthetic and natural polymers has been reported with some success. One of the methods of incorporation and direct immobilization is the electrodeposition of AgNP on different matrices. Silver electrocrystallization studies have been reported in the last decades, and the understanding of silver electrodeposition process is reached on plane electrodes. The role of electrode nature and the effects of ionic metal concentration determine the kinetic, morphology, nucleation and growth during the electrodeposition process [25–27]. In the same way, carbon nanomaterials such as graphene and MWCNT provide a nanostructure which may facilitate the AgNP immobilization and the established procedures can be transferred to design AgNP. Techniques as potentiostatic double pulse (PDP) and chronoamperometry [28] have been implemented to obtain silver nanoclusters in different modified carbon materials like graphene intercalated with poly(sodium 4-styrenesulfonate) [29, 30]. The electrodeposits obtained by these techniques on substrates like MWCNT are commonly in the range of 100 nm to 1 mm [28]. Likewise, the obtainment of AgNP of controlled sizes by applying potential sweeps has been achieved in the presence of the chloride ion, which acts as an "abrasive" that modulates the nanoparticle to the required size from massive silver electrodes to obtain AgNP of 10–100 nm [31, 32].

It is clear that the direct immobilization and the specific size of the AgNP become a challenge for the different applications, in addition to the growing interest of conjugating the activity of these nanoparticles with nanostructured carbon materials.

This chapter describes the obtainment of silver nanoparticles and silver nanoclusters (AgNC) by the electropolishing of micrometer silver obtained with electrodeposition on MWCNT film electrodes. The procedure involves anodic stripping voltammetry in the presence of chloride ions as a polishing agent. The effect of the MWCNT functionalization in the formation of AgNP and AgNC is shown. This method is a straightforward proposal which enables the redesign of micrometric Ag deposits to nanometric size and is adaptable to already existing electrodeposition procedures. An advantage of this method is the obtainment electrodes with AgNP or AgNC supported on MWCNT films ready for direct use in different applications.

2. General techniques

2.1. Silver electrodeposition

An electrochemical three-electrode cell was used, with a Pt mesh as a counter electrode, reference electrode sulfate saturated electrode (SSE, 0.644 V vs. NHE). As working electrodes, different carbon film electrodes (CFEs) were used, prepared from an ink containing MWCNT and Nafion (see below) and supported on glassy carbon (GC) as a current collector. The silver electrodeposition is carried out in 10 mM $AgNO_3$/1 M KNO_3, pH = 7 system. Different potential values were selected (between −0.05 and −0.100 V range) and applied a potential pulse during 30 s to obtained silver deposits on the different CFEs. The AgNP and AgNC were obtained through the remodeling and sculpturing of Ag deposits using anodic stripping voltammetry in a system free of silver ions:100 mM KCl/100 mM K_2HPO_4/KH_2PO_4, pH = 7

at 20 mV/s; the scan was initiated from open circuit potential (OCP) to positive direction. All the electrochemical measurements were taken with a Basic Autolab W/PGSTAT30 & FRA equipment using Nova 3.1 software; all the electrolytes were prepared with analytical-grade reagents and deionized water (18 MΩcm) using a Milli-QTM system.

2.2. Electrode preparation

The carbon film electrodes (CFEs) were prepared from an ink containing 3 mg MWCNT, 1 ml Nafion (0.05%) and isopropylic alcohol, mixed by sonication for 1 h. After, 3 µl of this ink was applied by dropping cast on GC and dried at room temperature. Before the dropping cast step, the GC surface was polished with fine 600 grit silicon carbide sandpaper, once rinsed GC was polished with cloth and alumina of 0.3 and 0.05 µm. MWCNTs were commercial with the following characteristics: 95% purity, 5–15 µm long, 2–7 nm ID and 10 nm OD (Nanostructured & Amorphous Materials Inc.). The MWCNTs were functionalized using reflux in 65% HNO_3 at different times: 2, 10 and 24 h. After the reflux step, the MWCNTs were washed with MiliQ water until pH 7 was reached, filtrated with 50 nm nitrocellulose filters. CFEs elaborated with functionalized MWCNT were identified in the manuscript as CFE2, CFE10 and CFE24, and the number corresponds to the reflux time.

2.3. CFE morphology and Ag particle size

Scanning electronic microscopy (SEM) is used to describe the morphology of the MWCNT as CFE after chemical treatment for every single reflux time, besides silver deposits were analyzed before and after electropolishing procedure. A scanning electron microscope (FE SEM Hitachi S-5500) was used to determine particle size, and distribution was obtained using the ImageJ 1.50i software.

### 2.4. X-ray photoelectron spectroscopy

Finally, an X-ray photoelectron spectroscopy (XPS) was used to perform the quantification of Cs1 and Os1, the spectra obtained from the average of three zones with a 400-μm^2 randomly selected area on the surface of each MWCNT material. The oxidize groups (hydroxyl, carbonyl and carboxyl) were quantified by deconvolution performed with GNUPLOT Free Software License 4.6 by multiple Gaussians fit.

3. Results and discussion

3.1. MWCNT morphology characterization

Figure 1 shows the SEM images corresponding to MWCNT with different reflux times (all images show the same magnification). The morphology and structure change as reflux time increases are presented. MWCNT in CFE2 shows few imperfections preserving structure possibly due to the treatment time reduction (**Figure 1A**). In the case of CFE10, the structures
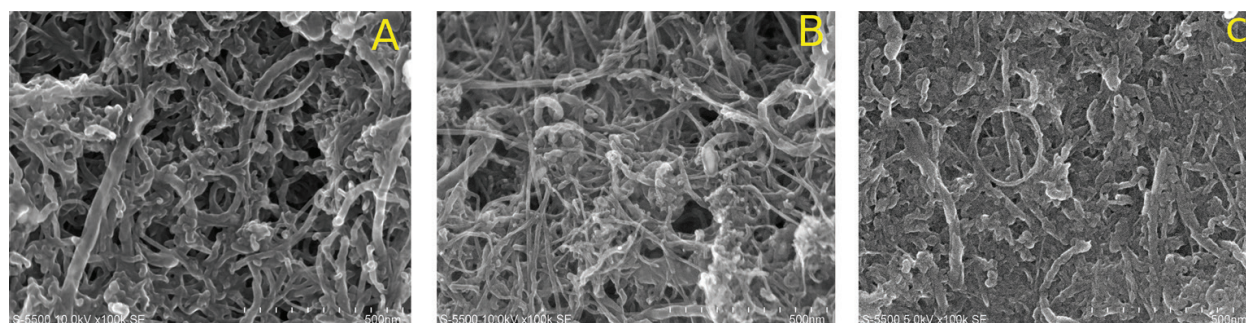
Figure 1. SEM images showing the morphology on: (A) CFE2, (B) CFE10 and (C) CFE24.

of MWNCT are preserved, but with lower diameter against CFE2, also many defects are observed on the MWNCT surface (**Figure 1B**). Finally, CFE24 presents a drastic loss of structure with aggregate formation tendency (**Figure 1C**). It is well known that long functionalization times affect MWCNT structure as has been already reported [33, 34].

3.2. X-ray photoelectron spectroscopy analysis

The MWCNT chemical surface composition was carried out through an XPS study. **Figure 2** shows the XPS spectra in the Cs1 and Os1 regions corresponding to MWCNT treated with acid reflux at different times. The intensity of Cs1 decreases as the reflux time increases, in contrast to the increase of Os1 peak in direct relation to the reflux time increase (**Figure 2A**, **B**). The deconvolution of Os1 for the MWCNT at 24 h is provided in **Figure 2C**. Four different peaks are presented in every O1s signal, and the functional group positions used for the deconvolution are C=O (531.2 eV), O-C=O* (531.6 eV), C-OH (532.8 eV) and O=C-O (534.5 eV) according to previous reports [33, 34]. **Table 1** shows the ratio of oxygenated group intensities on MWCNT with treatment against pristine MWCNT. At the treatment times of 2, 10 and 24 h in which case, the OH− and COO− groups are favored as time increases.

The XPS results show that reflux treatment provokes an increase in oxygen content with the concomitant carbon decrease; the only difference is the oxygenated functional groups content on every MWCNT. The generation of defects observed on SEM images is in direct correlation
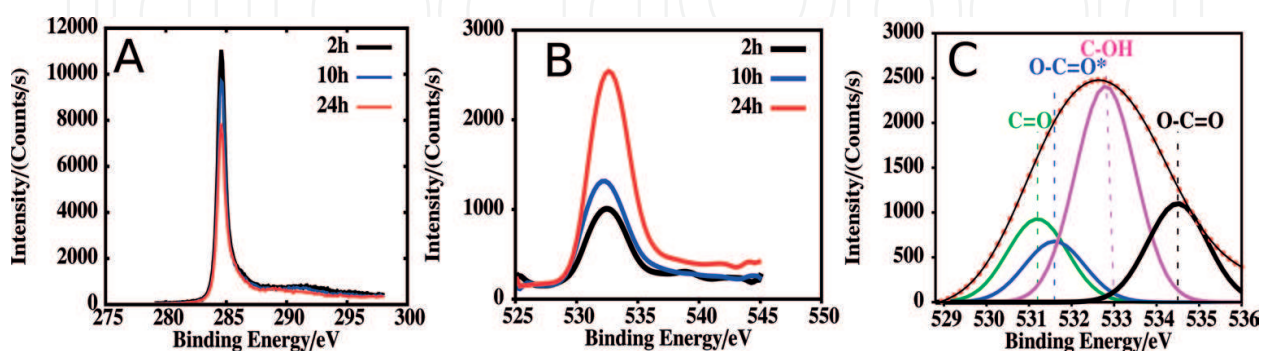
Figure 2. XPS spectra corresponding to MWCNT treated with acid reflux at different time. (A) Cs1, (B) Os1 and (C) deconvolution of Os1 for CFE24.

MWCNT functionalization time (h)	MWCNT$_f$/MWCNT$_p$		
	C-OH	C=O	COO⁻
2	1.88	0.27	0.46
10	2.90	0.99	1.94
24	5.15	2.21	3.57

Table 1. Relative appearance of functionalized groups against pristine MWCNT obtained by deconvolution of O1s shown in **Figure 2B**.

with the surface functionalization produced by this treatment. The relationship of these oxidized MWCNT surfaces on the silver electrodeposition process and remodeling will be discussed in further sections.

3.3. Electrodeposition of micro silver particles on MWCNT

With the aim of establishing the conditions for the silver electrodeposition process, a cyclic voltammetry study (CV) in 10 mM AgNO$_3$/1 M KNO$_3$ system was carried out to describe the potential range of silver electrodeposition at 20 mV/s. The scan initiates at open circuit potential (OCP) in the negative direction up to the potential limit of −0.6 V where the sweep direction is reversed to the uppermost potential at 0.6 V vs. SSE. **Figure 3** shows the responses corresponding to the different CFE (indicated in the figure); in all cases, two reduction steps are depicted by Red1 and Red2. In the reverse direction, the Ox1 peak is observed which corresponds to the redissolution process of the previously deposited silver. Noteworthy, density currents descend with MWCNT functionalization time; it is important to note that the deposition potentials are dependent on the electrode type. In **Table 2**, potential values for Red1 and Red2 are shown. This proves that silver deposition involved two processes. The
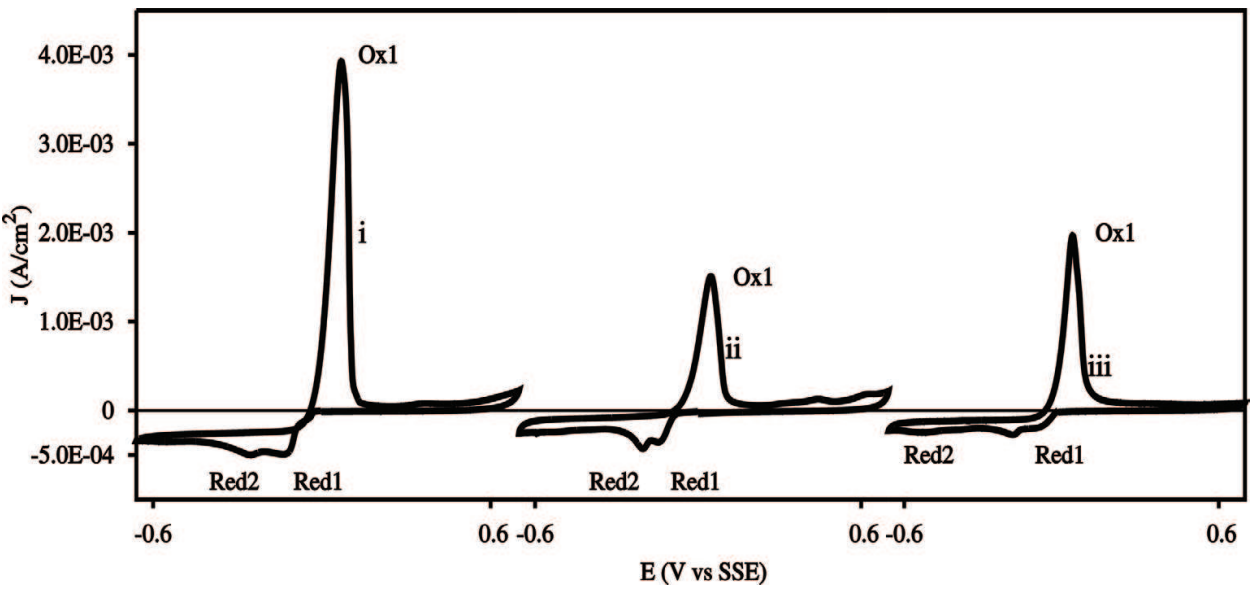
Figure 3. Cyclic voltammetry responses obtained in 10 mM AgNO$_3$/1 M KNO$_3$ system correspond to silver deposition on: (i) CFE2, (ii) CFE10 and (iii) CFE24. The scan started from OCP to negative direction at 20 mV/s, in the potential range −0.6 to 0.6 V vs. SSE.

Electrode	Red1(V vs. SSE.)	Red2 (V vs. SSE.)
CFE2	−0.133	−0.256
CFE10	−0.144	−0.200
CFE24	−0.186	−0.350

Table 2. Voltammetry parameters obtained of cyclic voltammetry studies for silver deposit.

lower reduction potentials observed at Red1 are possibly related to an energetically favor step due to more accessible physical sites. The higher electrodeposition potentials observed at Red2 indicate sites with difficult access for Ag^+ cation into the MWCNT matrix. The presented results show that there is a clear influence of the MWCNT surface chemistry on the silver electrodeposition process.

Considering the CV results discussed above, different potentials values were selected for Ag electrodeposition applying a 30 s pulse on every matrix. The electrodes obtained from this procedure are defined as $Ag°_{micro}$/CFE2, $Ag°_{micro}$/CFE10 and $Ag°_{micro}$/CFE24 for the applied potential of −0.083, −0.09 and −0.130 V vs. SSE, respectively. SEM images allow a description of the micrometric deposits; in all the cases, it is clear that MWCNTs are gradually covered by Ag° (**Figure 4A**-**C**). Silver intercalation is observed in MWCNT's matrix. In other areas, the presence of agglomerates is such that MWCNTs are no longer visible, and they are covered up in the silver deposits.

No matter the functionalization and the imperfections on the MWCNT surface, the micrometric silver electrodeposition was successful in three electrodes. The results presented here indicate that the silver micrometric electrodeposition process is independent of the MWCNT chemical surface moieties. Similar results have been previously reported, showing the micrometric silver on MWCNT after electrodeposition process which indicates that other steps may be needed to achieve AgNP by these techniques [29, 30]. An electropolishing procedure is proposed to take advantage of the different MWNCT chemical surface, and it is evinced that this procedure will act as a modulator for AgNP obtainment; the results are discussed in the next section as the following step after the electrodeposition process.
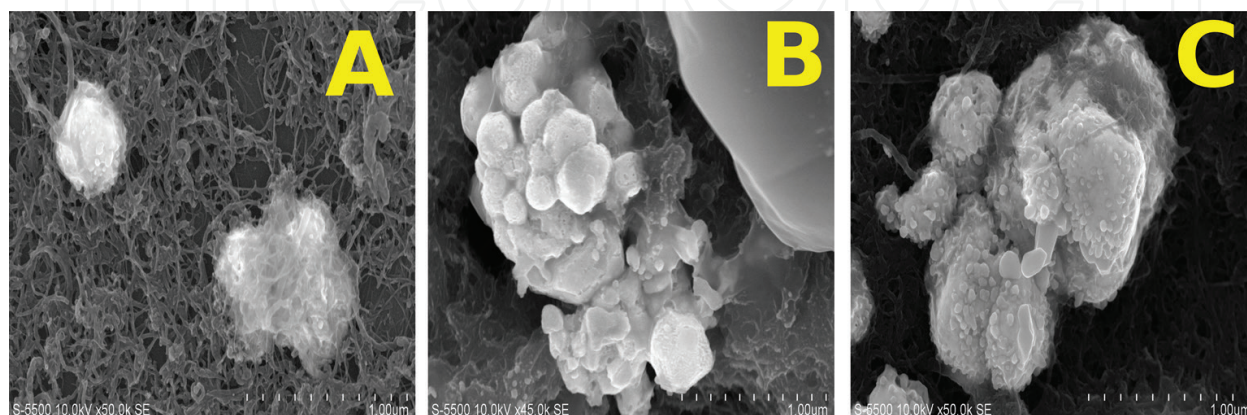
Figure 4. SEM images corresponding to (A) $Ag°_{micro}$/CFE2, (B)$Ag°_{micro}$/CFE10 and (C)$Ag°_{micro}$/CFE24.

3.4. Electropolishing of micrometric silver particles toward achieving AgNP and AgNC

To obtained AgNP and AgNC, a program of anodic stripping cycles in 100 mM KCl/100 mM K_2HPO_4/KH_2PO_4, pH = 7, at 20 mV/s was applied. **Figure 5** shows SEM images corresponding to AgNP obtained after the remodeling process. For AgNP/CFE2, dispersed particles of approximately 10 nm size (**Figure 5A**) are observed. On the other hand, for AgNP/CFE10 particles are around 20 nm, and a low population of them is observed (**Figure 5B**). Finally, the particles presented in AgNP/CFE24 are preferentially in the 10–20 nm range, and they are covering most of the MWCNT matrix (**Figure 5C**).

The formation of Ag nanocluster (AgNC) on MWNCT surface by electrochemical methods is scarcely reported [29, 30]. In our case, AgNC can be obtained from the electrodeposition process on CFE24 in the system 1 mM $AgNO_3$/1 M KNO_3 pH = 7 applying a − 0.070 V vs. SSE during 30 s. After anodic stripping voltammetry in similar experimental conditions described previously, AgNC/CFE24 was obtained (**Figure 6A**). The AgNC are well dispersed with a size between 1.2 and 1.8 nm (**Figure 6B**). Considering the atomic radii of Ag (0.144 nm), AgNC contains approximately 8–12 silver atoms. These AgNC are even smaller than the ones obtained by with poly(sodium4-styrenesulfonate) and oligonucleotides as intercalated agents, respectively [29, 30].

The advantage of the electrochemical method for the obtainment AgNP/CFE and AgNC/CFE is that these electrodes are ready for immediate use in different processes, such as electrocatalysis, specifically in the electrochemical reduction of CO_2 and O_2.

3.5. Steps involved in the formation of silver nanoclusters

What is the mechanism involved in the obtainment of AgNP and AgNC? When anodic stripping voltammetry was applied to the MWCNT with silver microdeposits, the Ag^+ is liberated to the bulk solution; in the presence of chloride anions, a AgCl(s) layer is formed (reaction 1).
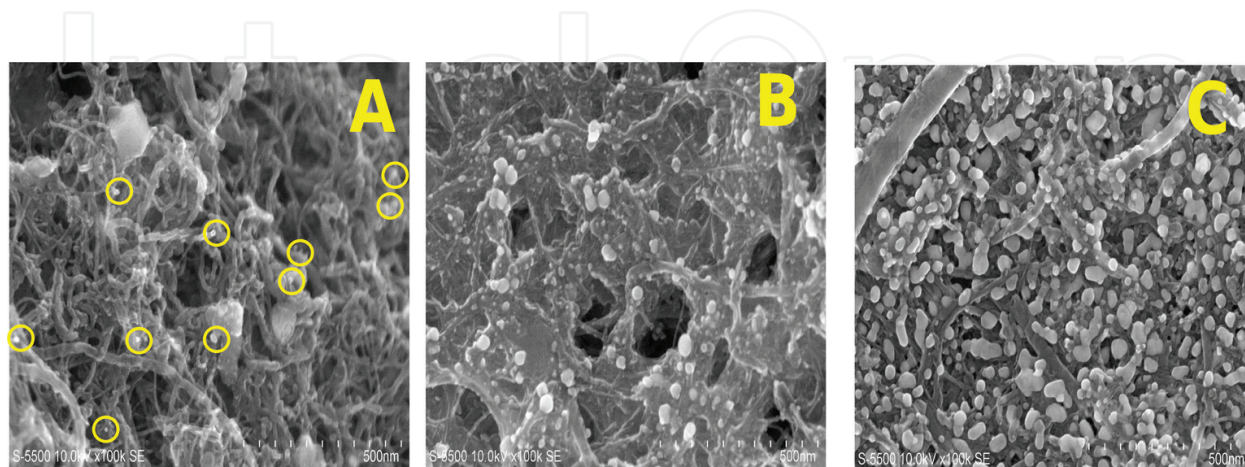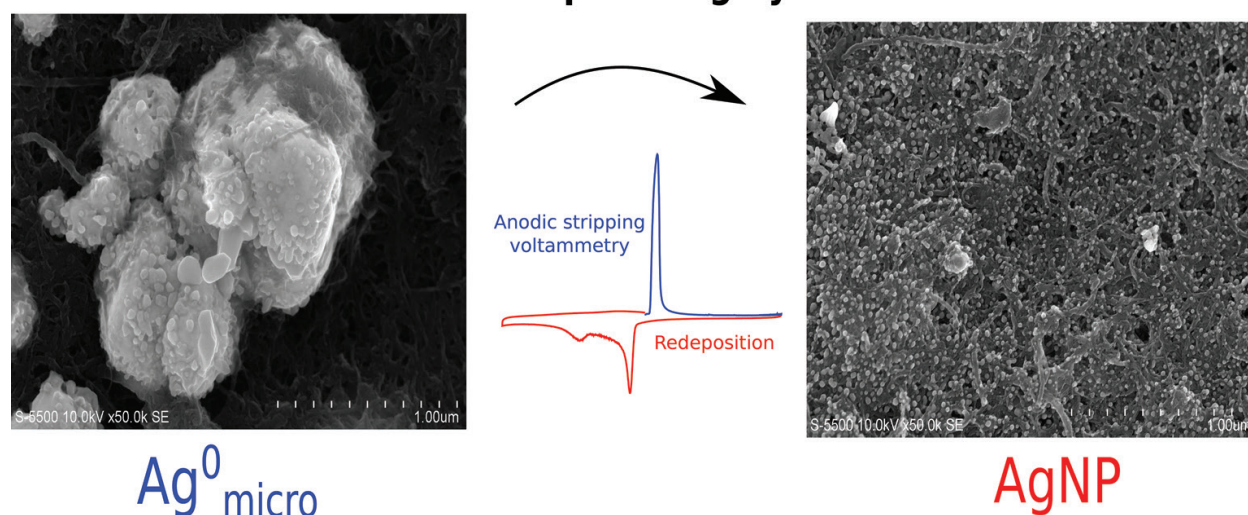

Figure 5. SEM images of AgNP supported on different CFE: (A) AgNP/CFE2, (B) AgNP/CFE10 and (C) AgNP/CFE24 after electropolishing by anodic stripping voltammetry procedure.
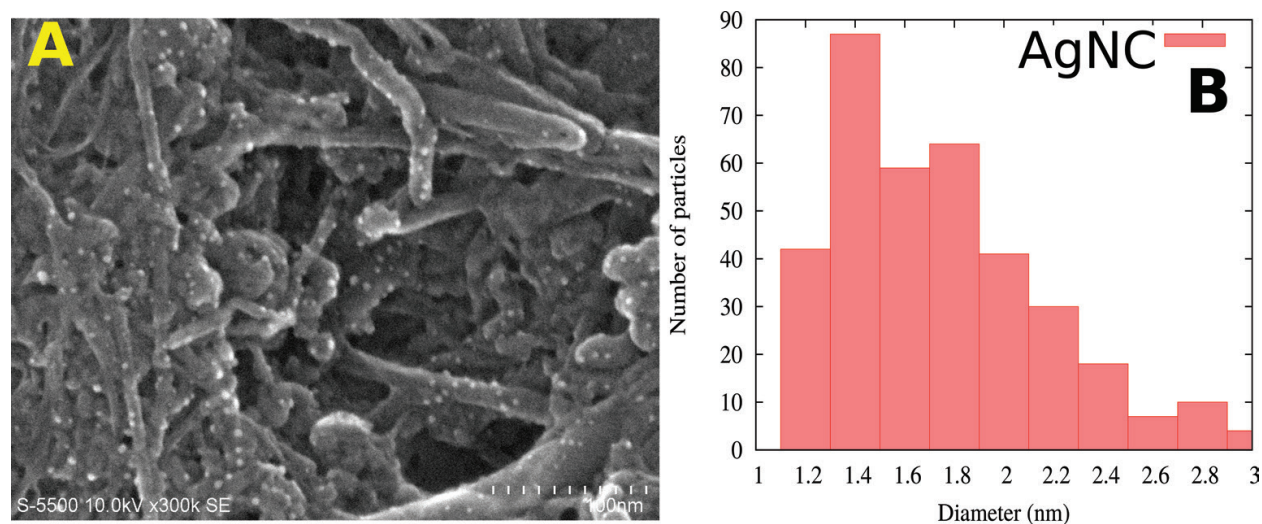
Figure 6. (A) SEM images of AgNC/CFE24 with deposit at 1 mM $AgNO_3$ after anodic stripping voltammetry procedure. (B) Particle distribution histogram.

Figure 7. Squematic representation of the electropolishing process for the obtainment of AgNP from Ag^0_{micro} in 100 mM $KCl/100$ mM K_2HPO_4/KH_2PO_4 pH = 7 at 20 mV/s.

The direction of the scan is reverse to promote the reduction of AgCl(s) to obtain AgNP or AgNC (reaction 2), and a representation of the process is presented in **Figure 7**. Then, the 10 consecutive stripping cycles allow the size modulation and the particle distribution of MWCNT matrix. The catalytic activity of these AgNP and AgNC has been recently reported for the electrochemical formate synthesis from CO_2 [35].

$$Ag^0_{micro} - e^- \rightarrow Ag^+ + Cl^- \rightarrow AgCl_{(s)} \tag{1}$$

$$AgCl_{(s)} + e^- \rightarrow Ag^0_{NP} + Cl^- \tag{2}$$

4. Conclusions

This chapter describes an outstanding methodology for the obtainment of in situ generating AgNP and AgNC on MWCNT film electrodes. This methodology allows the size modulation and the immobilization of the immediate application in catalytic processes such as the electrochemical reduction of O2 and CO2. The silver electrodeposition process is facilitated by the proper MWCNT functionalization; an original electropolishing process is applied for the AgNP and AgNC obtainment. This method markedly outstrips the existing procedures which are characterized by being more expensive and with multiple synthesis steps.

Acknowledgements

Author details

Andrés Alberto Arrocha Arcos and Margarita Miranda-Hernández*

*Address all correspondence to: mmh@ier.unam.mx

Institute of Renewable Energies, National Autonomous University of Mexico, Temixco, Morelos, México

References

[1] Kim C et al. Achieving selective and efficient electrocatalytic activity for CO_2 reduction using immobilized silver nanoparticles. Journal of the American Chemical Society. 2015;**137**:13844-13850. DOI: 10.1021/jacs.5b06568

[2] Sun R, Li SJ, Yao JL, Gu RA. Surface enhanced Raman spectroscopy and theoretical studies on the electrochemical transformation processes of 4-aminothiophenol on au electrode. Acta Chimica Sinica. 2007;**65**:1741-1745

[3] Cesarino I et al. Electrochemical degradation of benzene in natural water using silver nanoparticle-decorated carbon nanotubes. Materials Chemistry and Physics. 2013;**141**:304-309. DOI: 10.1016/j.matchemphys.2013.05.015

[4] Wan Q et al. In situ synthesized gold nanoparticles for direct electrochemistry of horseradish peroxidase. Colloids and Surfaces. B, Biointerfaces. 2013;**104**:181-185. DOI: 10.1016/j.colsurfb.2012.12.009

[5] Jin J et al. Nucleic acid-modulated silver nanoparticles: a new electrochemical platform for sensing chloride ion. The Analyst. 2011;**136**:3629-3634. DOI: 10.1039/c1an15283a

[6] Yu A et al. Silver nanoparticle-carbon nanotube hybrid films: Preparation and electrochemical sensing. Electrochimica Acta. 2012;**74**:111-116. DOI: 10.1016/j.electacta.2012.04.024

[7] Tsierkezos NG et al. Nitrogen-doped multi-walled carbon nanotubes modified with platinum, palladium, rhodium and silver nanoparticles in electrochemical sensing. Journal of Nanoparticle Research. 2014;**16**:1-13. DOI: 10.1007/s11051-014-2660-3

[8] Zamiri R et al. Laser based fabrication of chitosan mediated silver nanoparticles. Applied Physics A: Materials Science & Processing. 2011;**105**:255-259. DOI: 10.1007/s00339-011-6525-7

[9] Chen RH, Phuoc TX, Martello D. Effects of nanoparticles on nanofluid droplet evaporation. International Journal of Heat and Mass Transfer. 2010;**53**:3677-3682. DOI: 10.1016/j.ijheatmasstransfer.2010.04.006

[10] Noordeen S, Karthikeyan K, Parveen MN. Synthesis of silver nanoparticles by using sodium borohydride as a reducing agent. International Journal of Engineering Research Technology. 2013;**2**:388-397. DOI: 10.13140/2.1.3116.8648

[11] Van Hyning DL, Klemperer WG, Zukoski CF. Silver nanoparticle formation: Predictions and verification of the aggregative growth model. Langmuir. 2001;**17**:3128-3135. DOI: 10.1021/la000856h

[12] Soukupová J, Kvítek L, Panáček A, Nevěčná T, Zbořil R. Comprehensive study on surfactant role on silver nanoparticles (NPs) prepared via modified Tollens process. Materials Chemistry and Physics. 2008;**111**:77-81. DOI: 10.1016/j.matchemphys.2008.03.018

[13] Pal S et al. Site-specific synthesis and in situ immobilization of fluorescent silver nanoclusters on DNA nanoscaffolds by use of the tollens reaction. Angewandte Chemie - International Edition. 2011;**50**:4176-4179. DOI: 10.1002/anie.201007529

[14] Dondi R, Su W, Griffith GA, Clark G, Burley GA. Highly size- and shape-controlled synthesis of silver nanoparticles via a templated tollens reaction. Small. 2012;**8**:770-776. DOI: 10.1002/smll.201101474

[15] Huang L et al. UV-induced synthesis, characterization and formation mechanism of silver nanoparticles in alkalic carboxymethylated chitosan solution. Journal of Nanoparticle Research. 2008;**10**:1193-1202. DOI: 10.1007/s11051-007-9353-0

[16] Perelaer J, Klokkenburg M, Hendriks CE, Schubert US. Microwave flash sintering of inkjet-printed silver tracks on polymer substrates. Advanced Materials. 2009;**21**:4830-4834. DOI: 10.1002/adma.200901081

[17] Raghavendra GM, Jung J, Kim D, Seo J. Step-reduced synthesis of starch-silver nanoparticles. International Journal of Biological Macromolecules. 2016;**86**:126-128. DOI: 10.1016/j.ijbiomac.2016.01.057

[18] Kim B et al. Novel synthesis of porous silver nanostructures using a starch template and their applications toward plasmonic sensors. Chemphyschem. 2013;**14**:2663-2666. DOI: 10.1002/cphc.201300278

[19] Zaheer Z, Rafiuddin. Nucleation and growth kinetics of silver nanoparticles prepared by glutamic acid in micellar media. International Journal of Chemical Kinetics. 2012;**44**: 680-691. DOI: 10.1002/kin.20711

[20] Wallace JM et al. Silver-colloid-nucleated cytochrome c superstructures encapsulated in silica nanoarchitectures. Langmuir. 2014;**20**:9276-9281. DOI: 10.1021/la048478u

[21] Talekar S et al. Preparation of stable cross-linked enzyme aggregates (CLEAs) of NADH-dependent nitrate reductase and its use for silver nanoparticle synthesis from silver nitrate. Catalysis Communications. 2014;**53**:62-66. DOI: 10.1016/j.catcom.2014.05.003

[22] Syed B et al. Synthesis of silver nanoparticles by endosymbiont pseudomonas fluorescens CA 417 and their bactericidal activity. Enzyme and Microbial Technology. 2016;**95**: 128-136. DOI: 10.1016/j.enzmictec.2016.10.004

[23] Banerjee P, Satapathy M, Mukhopahayay A, Das P. Leaf extract mediated green synthesis of silver nanoparticles from widely available Indian plants: synthesis, characterization, antimicrobial property and toxicity analysis. Bioresource Bioprocess. 2014;**1**:3. DOI: 10.1186/s40643-014-0003-y

[24] Prasad R. Synthesis of silver nanoparticles in photosynthetic plants. Journal of Nanoparticles. 2014:1-8. DOI: 10.1155/2014/963961

[25] Miranda-Hernández M, González I. Effect of potential on the early stages of nucleation and growth during silver electrocrystallization in ammonium medium on vitreous carbon. Journal of the Electrochemical Society. 2004;**151**:C220. DOI: 10.1149/1.1646154

[26] Miranda-Hernández M, Palomar-Pardavé M, Batina N, González I. Identification of different silver nucleation processes on vitreous carbon surfaces from an ammonia electrolytic bath. Journal of Electroanalytical Chemistry. 1998;**443**:81-93. DOI: 10.1016/S0022-0728(97)00487-7

[27] Miranda-Hernández M, González I, Batina N. Silver electrocrystallization onto carbon electrodes with different surface morphology: Active sites vs surface features. The Journal of Physical Chemistry. B. 2001;**105**:4214-4223. DOI: 10.1021/jp002057d

[28] Ding YF, Jin GP, Yin JG. Electrodeposition of silver nanoparticles on MWCNT film electrodes for hydrogen peroxide sensing. Chinese Journal of Chemistry. 2007;**25**:1094-1098. DOI: 10.1002/cjoc.200790204

[29] Jin S et al. Stable silver nanoclusters electrochemically deposited on nitrogen-doped graphene as efficient electrocatalyst for oxygen reduction reaction. Journal of Power Sources. 2015;**274**:1173-1179. DOI: 10.1016/j.jpowsour.2014.10.098

[30] Lopes JH, Ye S, Gostick JT, Barralet JE, Merle G. Electrocatalytic oxygen reduction performance of silver nanoparticle decorated electrochemically exfoliated graphene. Langmuir. 2015;**31**:9718-9727. DOI: 10.1021/acs.langmuir.5b00559

[31] Hsieh YC, Senanayake SD, Zhang Y, Xu W, Polyansky DE. Effect of chloride anions on the synthesis and enhanced catalytic activity of silver nanocoral electrodes for CO_2 electroreduction. ACS Catalysis. 2015;**5**:5349-5356. DOI: 10.1021/acscatal.5b01235

[32] Zhang L, Wang Z, Mehio N, Jin X, Dai S. Thickness- and particle-size-dependent electrochemical reduction of carbon dioxide on thin-layer porous silver electrodes. ChemSusChem. 2016;**9**:428-432. DOI: 10.1002/cssc.201501637

[33] Wepasnick KA et al. Surface and structural characterization of multi-walled carbon nanotubes following different oxidative treatments. Carbon N. Y. 2001;**49**:24-36. DOI: 10.1016/j.carbon.2010.08.034

[34] Lehman JH, Terrones M, Mansfield E, Hurst KE, Meunier V. Evaluating the characteristics of multiwall carbon nanotubes. Carbon N. Y. 2011;**49**:2581-2602. DOI: 10.1016/j.carbon.2011.03.028

[35] Arrocha-Arcos AA, Cervantes-Alcalá R, Huerta-Miranda GA, Miranda-Hernández M. Electrochemical reduction of bicarbonate to formate with silver nanoparticles and silver nanoclusters supported on multiwalled carbon nanotubes. Electrochimica Acta. 2017;**246**:1082-1087. DOI: 10.1016/j.electacta.2017.06.147./j.electacta.2017.06.147